Classifying the Expansion Kinetics and Critical Surface Dynamics of Growing Cell Populations

M. Block,[1] E. Schöll,[1] and D. Drasdo[2,*]

[1]*Institut für Theoretische Physik, Technische Universität Berlin, 10623 Berlin, Germany*
[2]*INRIA, Paris-Rocquencourt, France, IZBI, University of Leipzig, Germany,*
and Mathematics Institute and Center for Systems Biology, University of Warwick, United Kingdom

(Received 13 September 2006; published 10 December 2007)

We systematically study the growth kinetics and the critical surface dynamics of cell monolayers by a class of computationally efficient cellular automaton models avoiding lattice artifacts. Our numerically derived front velocity relationship indicates the limitations of the Fisher-Kolmogorov-Petrovskii-Piskounov equation for tumor growth simulations. The critical surface dynamics corresponds to the Kardar-Parisi-Zhang universality class, which disagrees with the interpretation by Bru *et al.* of their experimental observations as generic molecular-beam-epitaxy-like growth, questioning their conjecture that a successful therapy should lead away from molecular beam epitaxy.

DOI: 10.1103/PhysRevLett.99.248101 PACS numbers: 87.18.Hf, 47.54.−r, 68.35.Ct, 89.75.Da

Model simulations of tumor growth and therapy have attracted wide interest [1] [2]. An important issue to which models can contribute is the classification of the tumor growth pattern by generic mechanisms at the level of the individual cell actions (migration, division, etc.). These actions subsume the effect of the molecular inter- and intracellular regulation. The models can serve to identify those cell activities whose modification would result in a maximal inhibition of multicellular growth and invasion, and thereby point to possible molecular drug targets. Bru *et al.* [3] analyzed the growth kinetics and critical surface dynamics of normal and malignant cell lines *in vitro* and *in vivo*. They quantified the dynamics of their surface by three *critical exponents* used to classify crystal growth phenomena into universality classes [4]. They found a generic linear growth phase of *in vitro* growing cell lines for large cell populations and a molecular-beam-epitaxy (MBE)-like dynamics of the population surface both *in vitro* and *in vivo*. Based on these findings they propose that a successful anticancer therapy should modify the universality class away from MBE mainly by changing cell migration [5].

In this Letter we analyze cell populations growing in $d = 2$ dimensions by a class of cellular automaton (CA) growth models on an irregular lattice by extensive computer simulations. CA cell growth models enjoy wide interest [6] since they permit to represent each cell individually at moderate computational expense. In our models cells can divide, push neighbor cells, and migrate which we believe is the minimum number of actions necessary to capture the growth behavior of cell populations in $d = 2$. By using the irregular lattice we ensure isotropy and homogeneity of the growth pattern avoiding artifacts from periodic lattices [7]. Also the expansion speed differs from results on periodic lattices. We systematically analyze our growth models with respect to the hopping rate, proliferation depth, and dispersion of the cell cycle time distribution and numerically derive a relation for the expansion velocity. It agrees with the traveling wave velocity of the Fisher-Kolmogorov-Petrovskii-Piskounov (FKPP) equation if growth is dominated by free cell migration [8]. The models reproduce the monolayer expansion kinetics experimentally found by Bru [3]. As in the Eden model [9] the critical surface growth dynamics suggests a Kadar-Parisi-Zhang (KPZ)-like [10] behavior over a wide range of parameters and for varying cell migration mechanisms including that proposed by Bru to explain the occurrence of MBE [3], supporting the critical comment in Ref. [11] on Bru's conjecture [3].

Our models are based upon the following rules:

[R1] *Lattice generation.*—Starting from a regular square lattice with spacing l, an irregular lattice $\underline{r}_i$ is generated by Delauney triangulation. A biological cell is represented as shown in Fig. 1(a) (white).

[R2] *Exclusion principle.*—Each lattice site can be occupied by at most one single cell.

[R3] *Proliferation depth.*—A cell can divide if and only if there is at least one free neighbor site within a circle of radius ΔL around the cell [Fig. 1(a), green].

[R4] *Cycle time.*—The cell cycle time τ' is Erlang distributed: $f(\tau') = \lambda_m(\lambda_m\tau')^{m-1}\exp\{-\lambda_m\tau'\}/(m-1)!$. Here, m is a shape parameter and $\lambda_m = m$ such that $\langle\tau'\rangle \equiv \tau = 1$.

[R5] *Cell migration.*—We consider four alternatives. R5(i) A cell moves with rate ϕ to a free neighbor site, irrespectively of the number of neighbor cells before and after its move. This mimics the case of no cell-cell adhesion. R5(ii) Cells move with rate ϕ if by this move the cell is not isolated. R5(iii) Cells move with a rate $\phi\exp\{-\Delta E/F_T\}$ with $\Delta E = E(t+\Delta t) - E(t)$, where Δt is the time step, $E(t)$ is the total interaction energy of the multicellular configuration, $F_T \sim 10^{-16}$ J is a "metabolic" energy [12], $\Delta E/F_T \sim \mathcal{O}(1)$–$\mathcal{O}(10)$ [2]. This induces migration towards locations with a larger number of neighbor cells as suggested in Ref. [3]. R5(iv) A migrating cell is able to push at most $\Delta\hat{L}$ cells aside with rate $\hat{\phi}$.

By [R1] we generate an irregular lattice with a symmetric cell area distribution sharply peaked around its average l^2 [Fig. 1(b)]. [R3] takes into regard that the growth speed

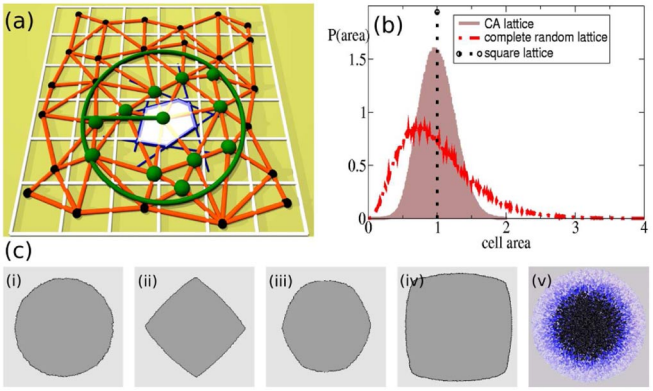

FIG. 1 (color online). (a) Construction of the CA lattice: one point (black, green) is placed in every square of a square lattice at a random position $\underline{r}_i$. A Voronoi tessellation is constructed from these points such that a cell i consists of all points in space that are closer to point $\underline{r}_i$ than to any $\underline{r}_k$ with $k \neq i$. The shape of a biological cell (white) is identified with the corresponding Voronoi polygon (blue lines). Polygons that share a common edge are defined as neighboring and connected by red lines (Delauney triangulation). (b) Probability density distribution of the cell area for the CA lattice in (a) (brown) and for a random initial distribution of points (red). (c) Cell cluster morphology for $m = 10^4$, $\Delta L = l$ on (i) the CA lattice in (a), (ii) square, (iii) hexagonal lattice, (iv) lattice with Moore neighborhood (nearest neighbors along the axes and the diagonals), (v) off-lattice cluster [2,20].

of cell populations is usually incompatible with the assumption that only cells at the border are able to divide (as in the Eden model [13], see [2]). Therefore, we assume that a dividing cell is able to trigger the migration of at most $\Delta L - 1$ neighbor cells into the direction of minimum mechanical stress [Fig. 1(a)]. If a cell divides, the local cell configuration is shifted and rearranged along the line that connects the dividing cell with the closest free lattice site within a circle of radius ΔL such that the latter is now occupied; then the original position of the mother cell and its cleared neighbor site are occupied by the two daughter cells [Fig. 1(a)]. This algorithm mimics a realistic rearrangement process that may occur from active cell migration as a response to a mechanical stimulus; cf. Ref. [14]. [R4] considers that experiments indicate a Γ-like distribution of the cell cycle controlled by cell cycle check points [15]. Isolated cells perform a random-walk-like motion (e.g., [16]). We consider different migration rules R5(i)–(iv) to comprise a class of potential models with biologically realistic behavior.

The model parameters are the average cell cycle time τ and its distribution $f(\tau')$ controlled by the parameter m, the migration rate ϕ, the proliferation depth ΔL, and, in case of an energy-activated migration rule, the energy E. Programmed cell death (apoptosis) can easily be integrated [17] but is omitted here. Rules [R1]–[R5] can be formalized by the master equation $\partial_t p(Z,t) = \sum_{Z'} W_{Z'\to Z} p(Z',t) - W_{Z\to Z'} p(Z,t)$. Here $p(Z,t)$ denotes the multivariate probability to find the cells in configuration Z at time t and $W_{Z'\to Z}$ denotes the transition rate from configuration Z' to configuration Z. A configuration $Z = \{\ldots, x_{i-1}, x_i, x_{i+1}, \ldots\}$ consists of local variables $x_i = \{0, 1\}$ with $x_i = 0$ if lattice site i is empty, and $x_i = 1$ if it is occupied by a cell. For the simulation we use the Gillespie algorithm [18]; i.e., the time step of the event-based simulation is a random number given by $\Delta t = -(1/W_{Z'}) \ln(1 - \xi)$. Here, ξ is a random number equidistributed in $[0, 1)$, $W_{Z'} = \sum_{\tilde{Z}(Z)} W_{Z'\to Z}$ is the sum of all possible events which may occur at time t. In $\tilde{Z}(Z)$ we assume that the rate at which a cell changes its state by a hop, a progress in the cell cycle, or a division is independent of the number of accessible states as long as at least one state, that is, one free adjacent lattice site in case of a hop and one free site within a circle of radius ΔL in case of a division, is accessible. This may be justified by noting that cells—in contrast to physical particles—are able to sense their environment and therefore the direction into which they can move.

We analyze the growth kinetics by the number of cells $N(t)$ and the radius of gyration $R_{gyr}(t) = \sqrt{\frac{1}{N}\sum_{i=1}^{N}[\underline{r}_i(t) - \underline{R}_0(t)]^2}$. $\underline{R}_0 = \frac{1}{N}\sum_{i=1}^{N} \underline{r}_i$ denotes the center of mass. For a compact circular cell aggregate (in $d = 2$), R_{gyr} is related to the mean aggregate radius $\bar{R}(t) = \frac{1}{2\pi}\int_0^{2\pi} R(\varphi, t) d\varphi$ (polar angle φ) by $\bar{R} = R_{gyr}\sqrt{2}$.

To interpret the rules and parameters of the CA model in terms of mechanisms we compare it with the stochastic single-cell-based off-lattice growth model in Ref. [2] (Fig. 2). In this model cell motion contains an active random component and a component triggered by mechanical forces between cells and between cells and the substrate [19]. A cell grows as long as thereby no cell is deformed or compressed too much, and it divides when it has doubled its size. As illustrated in Fig. 2 the lattice model is able to capture the behavior of the off-lattice model and the experimental findings in Refs. [3]. ΔL

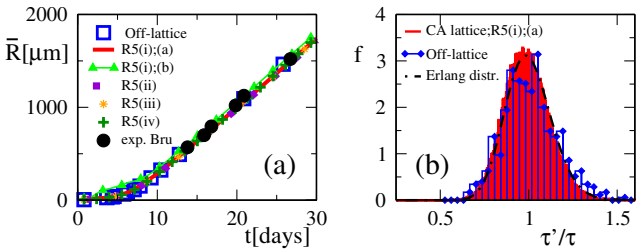

FIG. 2 (color online). (a) Mean radius $\bar{R}$ of the cell aggregate vs time t. Full circles: experiment for C6 rat astrocyte glioma cells [3]. Other symbols: CA simulations for different migration rules, R5(i) (a): $\Delta L = 9$, $\phi = 0$, R5(i) (b): $\Delta L = 1$, $\phi = 25$, R5(ii): $\Delta L = 8$, $\phi = 25$, R5(iii) $\Delta L = 9$, $\phi = 25$, $\Delta E/F_T = E_0 + nE_B$ with $E_B = 10$, n neighbors, $E_0 = 5$, R5(iv): $\Delta L = \Delta\hat{L} = 6$, $\hat{\phi} = 1$. (b) Cell cycle time distribution $f(\tau')$ for off-lattice model and CA growth model in comparison with Erlang distribution. ($m = 60$, $\tau = 19$ h, $l = 10$ μm [2]. ΔL and ϕ in units of l and τ^{-1}.)

controls the effective thickness of the proliferative rim; in the off-lattice model it depends on the mechanisms that control the proliferation by contact inhibition, on the material properties of the cell (the Young modulus, the Poisson number, etc.), and on the ability of a cells to move in response to a mechanical stimulus [2].

At large m the populations' border becomes smoother and its shape reflects the symmetry of the underlying lattice [Fig. 1(c) (ii)–(iv)], known as *noise reduction* [7]. Such lattice-induced asymmetries could significantly disturb the analysis of the surface growth dynamics in circular geometries. We have chosen an irregular lattice, in which such artifacts do not occur [Fig. 1(a) and 1(c)(i)]. Figure 3 shows a systematic study of the growth kinetics for free hopping [Rule R5(i)]. All quantities are plotted in multiples of the reference time scale τ and length scale l. Initially, the cell population size grows exponentially fast with $N(t) = N(0)\exp(t/\tau_{\text{eff}})$, where $\tau_{\text{eff}}^{-1} = (2^{1/m} - 1)m\tau^{-1}$ [20]. The duration of the initial phase increases with ΔL and ϕ. The growth law for the radius depends on ϕ. If $\phi = 0$, the initial expansion of the radius is exponentially fast, too. If $\phi > 0$, cells initially detach from the main cluster and the radius grows diffusively, with $\bar{R} \equiv \sqrt{2}R_{gyr} \propto \sqrt{A(\phi + 1/\tau_{\text{eff}})t}$, where $A \approx 1.2$ is a lattice-dependent fit constant [Fig. 3(a)]. For $t/\tau \leq 2$, $R_{gyr} \propto t$ [Fig. 3(a)]. This regime disappears for $N(0) \gg 1$ (see [20]). As soon as cells in the interior of the aggregate are incapable of further division the exponential growth crosses over to a linear expansion phase. Figure 3 shows v^2 versus $(\Delta L)^2$ (b), ϕ (c), and m for (d) for $N \sim 10^5$ cells. $v(m, \phi, \Delta L) = d\bar{R}/dt$. As $t \to \infty$,

$$v^2 \approx \{B^2([\Delta L'(\Delta L)]^2/\tau_{\text{eff}}^2 + \phi/\tau_{\text{eff}})\}, \quad (1)$$

$B \approx 1.4$ [lines in Fig. 3(b) and 3(c)]. We find $\Delta L'(\Delta L) \approx 1 + 0.6(\Delta L - 1)$ [21]. The model can explain the experimentally observed velocities for different cell lines, 1–11 μm/h [3]. For $\Delta L/\tau_{\text{eff}} \ll \sqrt{\phi/\tau_{\text{eff}}}$, $v^2 \propto \phi/\tau_{\text{eff}}$ as for the FKPP equation [8].

Next, to determine the universality class we determine the roughness exponent α and the dynamic exponent z from the dynamic structure function $S(k, t) = \langle R(k, t)R(-k, t)\rangle$ as in Ref. [3]. $R(k, t)$ is the Fourier transform of the local radius $R(s, t)$ and $\langle \ldots \rangle$ denotes the average over different realizations of the growth process. Here s is the arclength calculated from the mean distance $\bar{R}$ of the population boundary from the center of mass times the polar angle φ [3]. The Fourier transform includes the arclength interval $\Delta s = \bar{R}\Delta\varphi$ ($\Delta\varphi$ fixed) to include the boundary dilation as stressed in Ref. [22]. The third exponent, the growth exponent β, can be obtained from the scaling relation $\beta = \alpha/z$ or from the interface roughness $w \sim t^{\beta}$ [4]. For self-affine surfaces in absence of any critical length scale the dynamic structure function has the Family-Vicsek scaling form [23]:

$$S(k, t) = k^{-(2\alpha+1)}\tilde{s}(kt^{1/z}) \quad (2)$$

$$\tilde{s}(u = kt^{1/z}) = \begin{cases} \text{const.} & \text{if } u \gg 1, \\ u^{-(2\alpha+1)} & \text{if } u \ll 1. \end{cases} \quad (3)$$

At $u = 1$ a crossover occurs. For $u \gg 1$ curves measured at different times collapse onto a single line; at $u \ll 1$ they split. We have calculated $S(k, t)$ for rules R5(i) and $\phi \geq 0$, R5(ii) and R5(iii) (Fig. 4). The final cell population size was of $\mathcal{O}(10^5)$ cells, the typical size of the cell populations in Ref. [3]. All these results suggest KPZ-like dynamics with $\alpha = 1/2$, $z = 3/2$, and $\beta = 1/3$ rather than the MBE universality class, i.e., critical exponents $\alpha = 3/2$, $z = 4$, and $\beta = 3/8$ inferred in [3]. The parameter

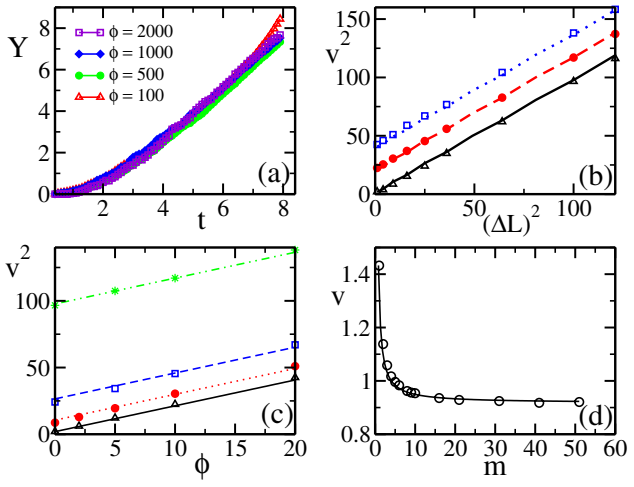

FIG. 3 (color online). (a) $Y = R_{gyr}^2/(\phi + 1/\tau_{\text{eff}})$ vs t for $m = 1$, $\Delta L = 1$ and different values for ϕ. (b)–(d) Growth in the linear expansion regime ($N \sim 10^5$). (b) Square of expansion velocity, v^2, vs square of the proliferation zone, ΔL^2 (△: $\phi = 0$, ○: $\phi = 10$, □: $\phi = 20$; $m = 1$). (c) v^2 vs ϕ (△: $\Delta L = 1$, ○: $\Delta L = 3$, □: $\Delta L = 6$, ☆: $\Delta L = 10$; $m = 1$). (d) v vs m ($\Delta L = 1$, $\phi = 0$). The lines are fits using Eq. (1). (Time and length in units of τ and l.)

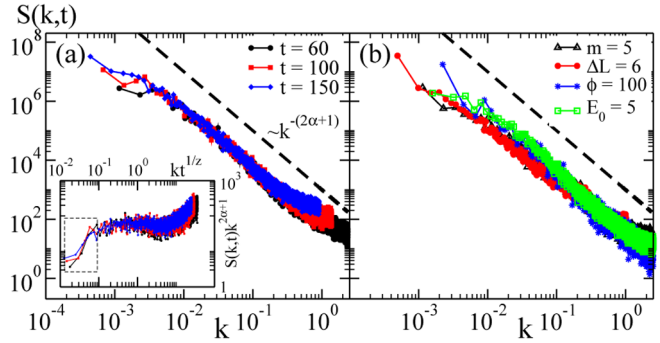

FIG. 4 (color online). (a) Dynamic structure function $S(k, t)$ vs k for [R5(i)], $\Delta L = 0$, $\phi = 0$, $m = 1$. Inset: scaling function $\tilde{s} = S(k, t)k^{2\alpha+1}$ vs $kt^{1/z}$ ($\alpha = 0.5$, $z = 3/2$). (b) $S(k, t)$ vs k for four alternative parameter sets: (A) △: $m = 5$ ($\Delta L = 0$, $\phi = 0$), (B) ○: $\Delta L = 6$ ($m = 1$, $\phi = 0$), (C) ☆: R5(ii) $\phi = 100$ ($m = 1$, $\Delta L = 0$), (D) □: R5(iii) $\Delta E/F_T$ as in Fig. 2(a) ($m = 1$, $\Delta L = 0$) [24]. The dashed lines are guides to the eye showing $\alpha = 0.5$. (Time and length in units of τ and l.)

range of $\phi \in [0, 100)$ captures most cell lines studied in Ref. [3] (for $l = 10$ μm, $\tau = 24$ h, $\phi = 100$ corresponds to a diffusion constant of $D \sim 10^{-11}$ cm^2/s).

In conclusion, we have analyzed the expansion kinetics and critical surface dynamics of cell aggregates in $d = 2$ by extensive computer simulations within a class of CA models avoiding symmetry artifacts from regular lattices. Our models differ by their migration rule R5(i)–(iv). For R5(i) cell adhesion is absent or negligible hence many isolated cells occur. For R5(ii) cells at the surface migrate randomly, for R5(iii) into local cavities; both are detectable by tracking of cells under the microscope [3]. For R5(iv), migrating interior cells push neighbor cells forward leading to a correlated movement of cells. The model parameters may be inferred either from macroscopic observations: τ_{eff} from the exponential growth of $N(t)$, $\Delta L'$ from Eq. (1), ΔL from $\Delta L'(\Delta L)$, and, for R5(i), ϕ from $Y(t)$ [Fig. 3(a)]; or microscopically: ϕ from tracking migrating isolated cells [16], ΔL, $\Delta L'$, τ, and m by cell cycle phase markers [15], E from adhesion experiments [19] and apoptosis [17] by TUNEL assay. The model rules and parameters may differ for each cell line and growth environment. If they are known, a classification of cell lines with regard to their growth behavior or predictions of spatial patterns at later times are feasible. Since some cell lines differ by mutations only, mutation effects on multicellular growth may be quantified [25]. In Ref. [26] the shape and velocity v of the front of glioma *in vivo* was calculated using the traveling wave velocity relation of the FKPP equation. However, Eq. (1) shows that this relation does not apply if ΔL is too large. Moreover, for a given v we found the front steepness increases with ΔL (not shown); if each parameter in Eq. (1) is known, both v and the front profile can be predicted. For some cancer cell lines, interior cells leave the monolayer and pile up. This can be captured by cell moves out of the layer; the effect should be as for apoptosis [17] so that the results in this Letter still apply for the basal layer. The critical surface dynamics found in our simulations does not comply with the interpretation of experimental observations by Bru *et al.* [3] even for the migration mechanism they suggested [R5(iii)] [27]. We propose to reanalyze the corresponding experiments and track the paths of marked cells.

M. B. acknowledges support within Sfb 296, D. D. by DFG (No. BIZ 6-1/1) and BMBF (HepatoSys Project No. 0313081).

*Corresponding author: dirk.drasdo@inria.fr

[1] R. A. Gatenby and P. K. Maini, Nature (London) **421**, 321 (2003); D.-S. Lee, H. Rieger, and K. Bartha, Phys. Rev. Lett. **96**, 058104 (2006).
[2] D. Drasdo and S. Höhme, Phys. Biol. **2**, 133 (2005).
[3] A. Brú, J. M. Pastor, I. Fernaud, I. Brú, S. Melle, and C. Berenguer, Phys. Rev. Lett. **81**, 4008 (1998); A. Brú, S. Albertos, J. L. Subiza, J. L. García-Asenjo, and I. Brú, Biophys. J. **85**, 2948 (2003).
[4] A.-L. Barabási and H. E. Stanley, *Fractal Concepts in Surface Growth* (Cambridge University Press, Cambridge, England, 1995).
[5] A. Brú, S. Albertos, J. L. García-Asenjo, and I. Brú, Phys. Rev. Lett. **92**, 238101 (2004); A. Bru, S. Albertos, F. Garcia-Hoz, and I. Bru, J. Clin. Res. **8**, 9 (2005).
[6] J. Krug and H. Spohn, in *Solids Far From Equilibrium: Growth, Morphology and Defects*, edited by C. Godreche (Cambridge University Press, Cambridge, England, 1991); J. Moreira and A. Deutsch, Advances in Complex Systems **5**, 247 (2002).
[7] M. Batchelor and B. Henry, Phys. Lett. A **157**, 229 (1991).
[8] J. Murray, *Mathematical Biology* (Oxford University Press, Oxford, 1989).
[9] E. Moro, Phys. Rev. Lett. **87**, 238303 (2001).
[10] M. Kardar, G. Parisi, and Y.-C. Zhang, Phys. Rev. Lett. **56**, 889 (1986).
[11] J. Buceta and J. Galeano, Biophys. J. **88**, 3734 (2005).
[12] D. Beysens, G. Forgacs, and J. Glazier, Proc. Natl. Acad. Sci. U.S.A. **97**, 9467 (2000).
[13] M. Eden, in *Proceedings of the 4th Berkeley Symposium on Mathematics and Probability*, edited by J. Neyman (University of California Press, Berkeley, 1961), pp. 223–239.
[14] A. R. Kansal, S. Torquato, G. R. I. Harsh, E. A. Chiocca, and T. S. Deisboeck, J. Theor. Biol. **203**, 367 (2000).
[15] J. A. Smith and L. Martin, Proc. Natl. Acad. Sci. U.S.A. **70**, 1263 (1973).
[16] M. Schienbein, K. Franke, and H. Gruler, Phys. Rev. E **49**, 5462 (1994).
[17] We mainly found a rescaling of the proliferation rate τ^{-1} to $\tau^{-1} - \gamma$ if apoptosis also occurs in the proliferative rim, and otherwise no effect (γ is the apoptosis rate).
[18] D. T. Gillespie, J. Comput. Phys. **22**, 403 (1976); also Bortz-Kalos-Lebowitz algorithm: A. B. Bortz, M. H. Kalos, and J. L. Lebowitz, J. Comput. Phys. **17**, 10 (1975).
[19] Y.-S. Chu, S. Dufour, J. P. Thiery, E. Perez, and F. Pincet, Phys. Rev. Lett. **94**, 028102 (2005).
[20] D. Drasdo, Advances in Complex Systems **8**, 319 (2005).
[21] If a cell senses free neighbor sites within ΔL before it reenters the cell cycle instead of before division, $\Delta L' = \Delta L$.
[22] J. Ramasco, J. Lopez, and M. Rodriguez, Phys. Rev. Lett. **84**, 2199 (2000).
[23] F. Family and T. Vicsek, J. Phys. A **18**, L75 (1985).
[24] We have also tested $S(k, t)$ versus k for R5(i), $\Delta L = 0$, $\phi = 10$, $m = 1$ and found $\alpha \simeq 0.5$.
[25] E.g., normal 3T3 cells grow slower than *K*-ras (transformed) 3T3 cells [3] where the Ras protein is permanently activated promoting signaling in different signal tranduction pathways. Knowing the rules and parameters of our model may permit to quantify the cellular and multicellular growth phenotype of different Ras variants.
[26] H. L. P. Harpold, E. C. Alvord, Jr., and K. R. Swanson, J. Neuropathol. Exp. Neurol. **66**, 1 (2007).
[27] We found that $S(k, t)$ suggests MBE-like behavior if points are added between the centers of the surface cells and the division by the growing perimeter is missed out.